

Realizing Symmetry-Breaking Architectures in Soap Films

Original

Realizing Symmetry-Breaking Architectures in Soap Films / Bergamasco, Luca; Chiavazzo, Eliodoro. - In: PHYSICAL REVIEW LETTERS. - ISSN 1079-7114. - ELETTRONICO. - 132:(2024), pp. 1-6. [10.1103/PhysRevLett.132.028201]

Availability:

This version is available at: 11583/2984951 since: 2024-01-10T17:10:25Z

Publisher:

APS

Published

DOI:10.1103/PhysRevLett.132.028201

Terms of use:

This article is made available under terms and conditions as specified in the corresponding bibliographic description in the repository

Publisher copyright

AIMS postprint/Author's Accepted Manuscript [con art. gia' pubblicato]

This article has been published in a revised form in PHYSICAL REVIEW LETTERS {<http://dx.doi.org/{dc.identifier.doi}>}. This version is free to download for private research and study only. Not for redistribution, re-sale or use in derivative works.

(Article begins on next page)

Realizing Symmetry-Breaking Architectures in Soap Films

Nidhi Kaul,^{1,||} Luca Bergamasco,^{2,||} Hongwei Song,^{1,||} Thijs Varkevisser,^{3,||} Agnese Amati,⁴ Gabriele Falciani,² Cees J. M. van Rijn,³ Eliodoro Chiavazzo,^{2,*} Indraneel Sen,^{5,†} Sylvestre Bonnet,^{4,‡} and Leif Hammarström^{1,§}


¹*Department of Chemistry, Ångström Laboratory, Uppsala University, Box 523, 751 20 Uppsala, Sweden*

²*Department of Energy, Politecnico di Torino, Torino 10129, Italy*

³*Nanotechnology and Microfluidics, Institute of Physics, University of Amsterdam, Science Park 904, 1098XH Amsterdam, The Netherlands*

⁴*Leiden Institute of Chemistry, Leiden University, Einsteinweg 55, 2333 CC Leiden, The Netherlands*

⁵*Wasabi Innovations Ltd., Boulevard “Shipchenski Prohod” 18, Block A, Floor 3, Office 9, Slatina, Galaxy Business Center, 1113 Sofia, Bulgaria*

 (Received 31 October 2022; revised 2 October 2023; accepted 11 December 2023; published 10 January 2024)

We show here that soap films—typically expected to host symmetric molecular arrangements—can be constructed with differing opposite surfaces, breaking their symmetry, and making them reminiscent of functional biological motifs found in nature. Using fluorescent molecular probes as dopants on different sides of the film, resonance energy transfer could be employed to confirm the lack of symmetry, which was found to persist on timescales of several minutes. Further, a theoretical analysis of the main transport phenomena involved yielded good agreement with the experimental observations.

DOI: [10.1103/PhysRevLett.132.028201](https://doi.org/10.1103/PhysRevLett.132.028201)

Long ago, Weyl expressed the sentiment: “All *a priori* statements in physics find their origin in symmetry” [1]. Indeed, our very existence is a by-product of broken symmetries at the subatomic level [2], even as the laws which govern us are engendered in conservation thereof [3,4]. Nature makes a compelling case for symmetry-breaking constructs to realize function: asymmetric inside-outside arrangement of membrane-bound proteins on a thylakoid membrane enables the utilization of proton gradients to drive life-sustaining reactions such as synthesis of ATP. More generally, symmetry-breaking arrangements of phospholipids lead to transmembrane electric and chemical potential gradients, resulting in different propensity for interaction with substances on the opposite sides [5,6], thus driving biological function. The retinal distribution of rods and cones is also radially asymmetric, yet another well-known example of a mesoscopic symmetry-breaking supramolecular arrangement extant in nature [7,8].

Soap films and bubbles have intrigued children and brilliant minds alike for centuries [9–11]; they poetically straddle the interface of art [12] and science, with interests spanning from their interference fringes to their rupture behavior and longevity [13,14]. These inconspicuous dynamical fluid structures bear a resemblance to aforementioned biological membranes—not in the least when it comes

to beauty and complexity. Considered as thin layers of liquid stabilized by amphiphilic surfactant molecules [15], soap films bear topological resemblance to natural lipid bilayers enclosing an aqueous phase, e.g., thylakoids. Concurrently, the so-generated air-water interfaces also likens them to cell walls.

From this perspective, the possibility of generating a symmetry-breaking architecture on opposite interfaces of otherwise intrinsically symmetric soap films is an intriguing proposition. If realized, it would bring soap films closer to natural membranes, and open possibilities for novel functions. Furthermore, the aqueous and surfactant phases that comprise soap films can be tuned by dopants, influencing their properties; see, e.g., recent reports on how surfactants may control the strength of the strong electric field at the gas-water dielectric interface [16], potentially leading to ultrafast reactions compared to homogenous bulk conditions [17]. Other potential applications can be envisioned in the context of gas permeation through soap films, where surfactants can fine-tune different permeability values at the two interfaces [18] and the recent concept of photosynthetic soft membranes [19]. These favorable prospects taken together with their low cost, easy generation, and scalability, could make soap films with mesoscopic tailored supramolecular arrangements—much as proteins are preferentially arranged in lipid bilayers—robust building blocks for future applications.

In this Letter, we present therefore, to the best of our knowledge, first proof of a symmetry-breaking supramolecular arrangement in soap films on the mesoscopic scale, by employing amphiphilic fluorescent molecular probes as dopants, see Fig. 1.

Published by the American Physical Society under the terms of the Creative Commons Attribution 4.0 International license. Further distribution of this work must maintain attribution to the author(s) and the published article's title, journal citation, and DOI. Funded by Bibsam.

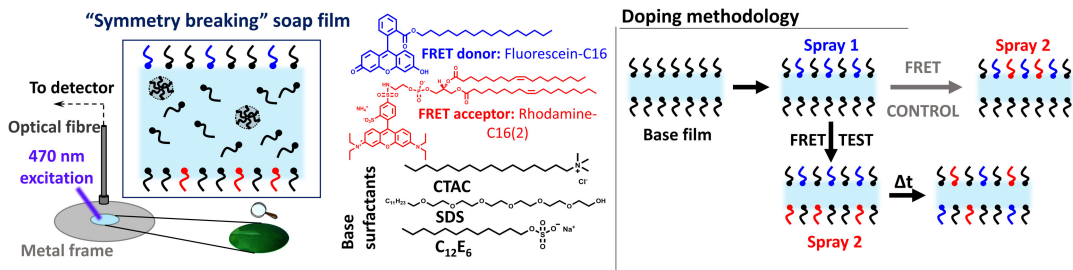


FIG. 1. *Left*: Molecular structures of amphiphilic fluorescein (blue), rhodamine (red), and different base surfactants (black) used in this study, together with a schematic depiction of the setup used for measurements and a cartoon depiction of the envisioned symmetry-breaking soap film. *Right*: Schematic depiction of the experiments used in this work to distinguish a symmetric and symmetry-breaking soap film.

The molecules chosen were surface-active analogs of fluorescein and rhodamine, a classic donor-acceptor pair with significant spectral overlap to undergo Förster resonance energy transfer (FRET). Upon confining the dyes in micelles of the nonionic surfactant $C_{12}E_6$ (hexaethylene glycol monododecyl ether) with a hydrodynamic radius ~ 3.7 nm [20], efficient ($>80\%$) energy transfer could be observed at an average occupancy of ~ 1 /micelle of each dye. This was found consistent with a Förster radius (corresponding to 50% efficiency of energy transfer) of approximately 5.5 nm for related fluorescein-rhodamine couples [21], thus validating the choice of dopants.

Well established as a “molecular ruler” [22], FRET is very sensitive to the distance between donor and acceptor, with efficiency falling off as the sixth power of the distance. Occurrence of FRET, therefore, is typically limited to donor-acceptor distances <8 nm. Soap films, during the experiments, had thicknesses exceeding 500 nm, which could be independently verified using both film rupture velocity measurements and nonobservation of interference colors. A set of FRET experiments, as illustrated in the right panel of Fig. 1, can therefore be rationalized to test the symmetry-breaking hypothesis in such films. Doping the donor and acceptor on different sides of the soap film should preclude FRET, presenting direct evidence of symmetry-breaking on the measured timescales. Conversely, FRET can be expected to occur in a facile way if the dopants migrate between the different interfaces *or* if they are deliberately doped on the same side (control).

Given the flexible and dynamical nature of the fluid thin film, conventional doping methods such as drop casting or injection with a syringe tip proved ineffective. Large turbulence generated in the mesoscopic film due to the impinging drop was found sufficient to trivially mix the dyes. Consequently, the donor, fluorescein, and acceptor, rhodamine, were doped on either different or same sides of a soap film by employing a Rayleigh spray nozzle (Fig. S20 [23]). This enabled the generation an aerosol of the dye solution [10 μ M of the dye at different concentrations of the base surfactant, with the latter typically at 1 or 10 times the critical micellar concentration (CMC)].

The mean droplet size was about 20 μ m, and deposition occurred on the same or different sides of the soap film. In all cases, the soap film was made from the same base surfactant concentration as used for the dye solution. This method allowed for introduction of the dopants with negligible mechanical perturbation of the soap film membrane (see below). The three base surfactants tested were $C_{12}E_6$, sodium dodecyl sulphate (SDS), and cetyltrimethylammonium chloride (CTAC), presenting cases of a neutral, anionic, and cationic surfactant, respectively.

The method of using FRET to detect migration of dyes from one side to the other side of the film could be validated via the control (Fig. 2, first column) where 10 μ M solutions of the donor and acceptor were sprayed on the same side of the film. Energy transfer could be readily confirmed between them by direct observation of the acceptor’s spectral band at 590 nm while exclusively exciting the donor at 470 nm.

Upon spraying 10 μ M solutions of the donor and acceptor on different sides of the soap film and excitation of the donor at 470 nm, persistent symmetry breaking on the timescale of at least several minutes could be observed for base surfactants CTAC and SDS (Fig. 2, middle column, top and bottom; concentration of CTAC = 1.1 mM, and SDS = 8 mM, i.e., 1 CMC), as evidenced by the sole presence of the donor peak (centred at around 535 nm) and absence of any acceptor peak (expected at 590 nm) in the fluorescence spectra. For the case of base surfactant $C_{12}E_6$, however, no symmetry breaking could be observed at any concentration, see Fig. S4 in Ref. [23]. Finally, upon spraying the dopants on different sides of the film, only partial symmetry breaking could be observed in CTAC and SDS when their concentration was 10 times the CMC (Fig. 2, last column).

Taken together, the data—qualitatively similar for both surfactants SDS and CTAC—establish symmetry breaking on the timescale of several minutes when the base surfactant concentration is 1 CMC, limited only by the stability of the soap film itself. Meanwhile, the nonobservance of symmetry breaking in the experiments conducted at 10 CMC is also amenable to a simple explanation: micellar

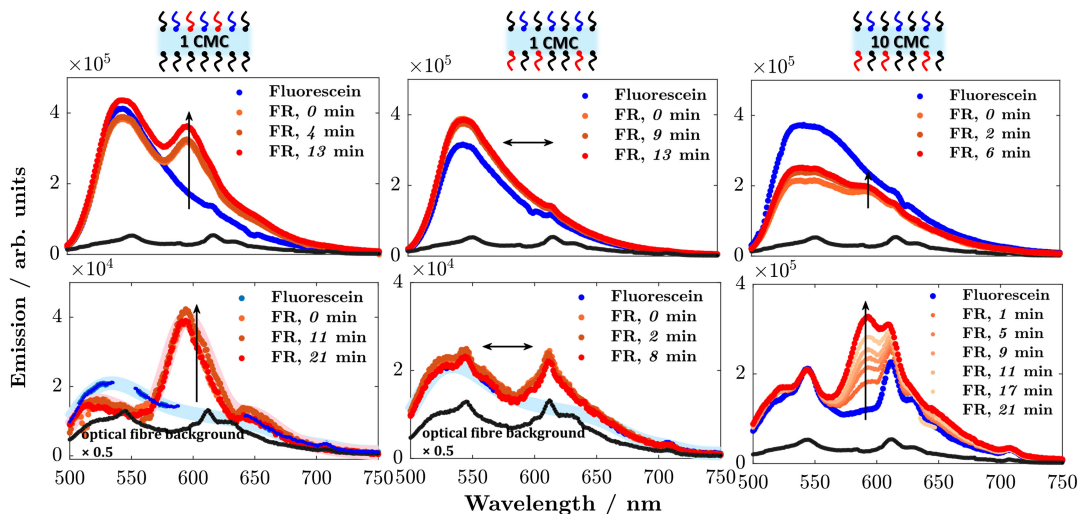


FIG. 2. Steady state luminescence data recorded for the amphiphilic dyes (10 μM solutions in the base surfactant) spray-doped on soap films of CTAC (top panel) and SDS (bottom panel) made from the same base surfactant. Excitation wavelength was 470 nm where the donor fluorescein was predominantly excited. *Top left*: Fluorescein and rhodamine sprayed on the same side of the soap film (base surfactant CTAC; concentration = 1.1 mM, 1 CMC). Immediate appearance of the rhodamine acceptor fluorescence peak at 590 nm clearly indicates the occurrence of FRET in the control, validating the method. *Top middle*: Fluorescein and rhodamine sprayed on different sides of the soap film (base surfactant CTAC, 1 CMC). Only fluorescein fluorescence ($\lambda_{\text{max}} \approx 535$ nm) is observed; absence of any acceptor peak indicates persistent broken symmetry for at least 13 min, when the film broke. *Top right*: Fluorescein and rhodamine sprayed on different sides of the soap film (base surfactant CTAC; concentration = 11 mM, 10 CMC). *Bottom panel*: Same as the top panel, but with base surfactant SDS. *Note*: Signals in SDS are an order of magnitude lower than CTAC; the Fluorescein signal therefore nearly coincided with the background and has been plotted as a blue shaded line after correcting the data for background. SDS data at 10 CMC has been normalized to the fiber background at 540 nm for clearer depiction of the acceptor intensity increment.

solubilization is likely responsible for transport of the dopants across the aqueous phase, and symmetrizes the interfaces. This interpretation is justified by the fact that the majority of dyes can be expected to be present in base surfactant micelles and not as monomers at the interface, in 10 CMC of the base surfactant. A distinct time evolution is also observed in the spectra at 10 CMC for SDS (Fig. 2, bottom right), which we tentatively attribute to a combined effect of micelle-assisted dopant transport and dye deaggregation.

Time-resolved lifetime measurements reveal that dynamic quenching is insignificant in the control when fluorescein and rhodamine are sprayed on the same side of the film (Fig. S12 [23]), consistent with the approx. 4 ns lifetime of the donor, during which the extent of diffusion is expected to be minimal. The largely static quenching (quenching sphere of action) is manifest in the lifetime decay becoming biexponential [46]. Estimates of the extent of dye loading per spray using absorption measurements suggest nearly complete geometric surface coverage by the dopants: therefore, the relatively smaller extent of observed quenching ($\sim 5\%$) points to the presence of molecular aggregates and interactions between them. This notion is corroborated by the observation of increased self-quenching instead of energy transfer upon substantial increase of the acceptor loading, and an overall lowering of the signal intensity (Fig. S8 [23]).

We observe that timescales for the emission intensity increase at the single interface are found to be consistent with the slowest processes associated with the envisioned main transport phenomena involved (Fig. S19 [23]). Here, the overall doping process can be thought to be characterized by four critical steps: (a) the deposition of the spray droplet on the soap film, (b) micelle and/or monomer diffusion to the contact area of the droplet and soap film, (c) diffusion of the dopant within the micelle and subsequent overcoming of the Gibbs free energy barrier for deposition on the soap film surface, and finally, (d) mixing of the dopant molecule at the interface under the effect of Marangoni flows. As detailed in the Supplemental Material [23], when using surfactant of the same nature for both the doping solution and the film, upon the spray, self-standing droplets can be envisioned in the vicinity of monolayers. Under such an assumption, the slowest transport phenomena can be associated with the first three steps and estimated in the order of minute timescales, while the last process involving mixing of the monomers on the interface after deposition may take seconds or shorter.

Micellar solubilization was found to be a key factor controlling the symmetry breaking, necessitating the use of CMC or sub-CMC concentrations of base surfactants. The use of such concentrations was not sufficient, however, as was found for the case of $C_{12}E_6$, where no symmetry-breaking was observed even at 1 CMC. This highlights that

both the nature and concentration of base surfactant are important.

The contrast is also found when considering physical properties: CTAC and SDS are charged as opposed to the neutral $C_{12}E_6$, and the resulting electrostatic interactions can be expected to contribute to both the droplet-deposition and coalescence dynamics. Indeed, it could be confirmed that symmetry could not be broken if dopant solutions in CTAC were sprayed on a soap film made of SDS, even at 1 CMC, owing to the opposite charges. Further, the base surfactant impacts the extent of dye aggregation: much higher signals observed in CTAC are consistent with the cationic surfactant both assisting in breaking up aggregates and stabilizing the anionic species of fluorescein, which is known to have almost 3 times the quantum yield of the neutral molecule (with the latter being the dominant species in SDS and $C_{12}E_6$) [47,48].

Video acquisitions were performed using a high-speed camera to directly observe the dopant-droplet coalescence dynamics with the soap film, in the same conditions as the FRET experiments. A snapshot is presented in Fig. 3 (full videos in the Supplemental Material [23]). After the spray—consisting of droplets with a mean diameter of around 20 μm —droplet diameters of up to 60 μm could be observed prior to impact with the soap film, due to coalescence events during the trajectory. Droplet impact with the film was characterized by the formation of fast capillary waves with a radial propagation velocity in the order of 3 m/s. The resultant amplitude of these waves could be estimated at around 1 μm . The fine spray therefore prevents symmetrization by trivial impact mixing for the two sides of soap films studied herein, since their thicknesses range from 5–7 μm . Droplets both bounce off of and coalesce with the soap film postimpact, with the latter characterized by the formation of a liquid bridge (neck) followed by radial spreading. Further, the radius of the surfactant deposition zone was found to scale as $r \sim t^\alpha$, consistent with the literature.

Thermodynamically, a mechanically “nonperturbative” condition may be discussed to corroborate the observations.

The ratio between the induced free energy change associated with a single droplet coalescence process and the initial free energy of the soap film before coalescence is plotted for the system in Fig. 4, and shows that up to around 100 μm droplet diameter, the induced free energy change is very small compared to that of the soap film, whereas it steps up quickly for larger droplets and eventually becomes comparable for mm-sized droplets. Accordingly, we have observed that the dissymmetry is destroyed upon use of such macrodroplets for doping, thus associating the nonperturbative condition with the minimal free energy change induced by the fine spray. For the case of multiple coalescence events involved in the adopted spray, the time lag among such events may be sufficient to minimize the cumulative free energy step in the system. Finally, surface tension measurements indicate small but measurable surface energy differences (up to 6%) between the differently doped monolayers (Ref. [23], pp. 31–33). In addition, the concentration differences of fluorescein and rhodamine give a chemical potential gradient for these species across the film. The resulting difference in chemical potential between the two sides can therefore be thought to drive symmetrization of the two sides. The persistence of symmetry breaking on minute timescales despite the few micron film thickness can, thus—in a kinetic perspective—be attributed to the insolubility of the dopants.

To conclude, we have demonstrated the construction of a mesoscopic symmetry-breaking supramolecular arrangement on soap films, on timescales substantially long enough to allow for meaningful chemistry to take place. Further, we have experimentally delineated critical factors enabling the symmetry breaking: optimal base surfactant and concentrations for film preparation, and a mechanically nonperturbative and scalable spray technique for film doping. Using a multiscale model of the critical transport phenomena, insight was gained into the dynamics, where droplet deposition, coalescence, and dye deaggregation could be isolated as rate-limiting steps. The deposition and coalescence steps could be directly observed experimentally; together with a free-energy change calculation for the

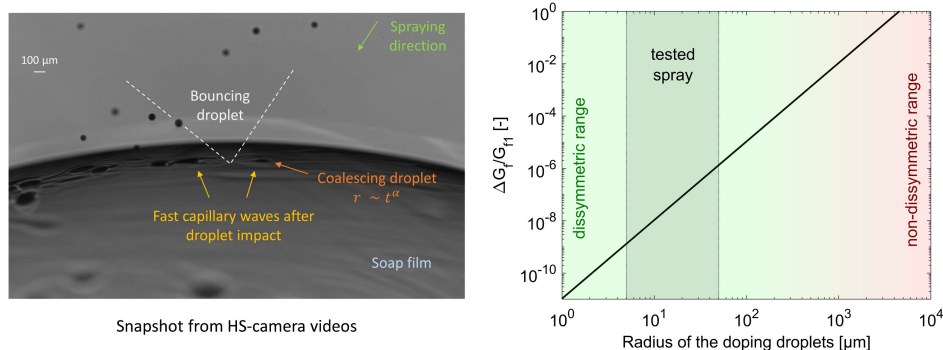


FIG. 3. *Left*: Selected frame from high-speed camera measurements to study droplet coalescence dynamics in the soap films. *Right*: Dimensionless free energy change in the soap film induced by the droplet coalescence process as a function of the droplet diameter.

coalescence process, quantitative estimates of permissible droplet sizes for symmetry breaking could be made, highlighting the importance of the doping methodology. Finally, the evaluated timescales of these processes—on the order of several minutes—were found in good agreement with observations, validating the proposed model. Inasmuch as all calculations in the latter have been undertaken with robust estimates of the physical parameters from the literature, the results can be regarded as general.

Langmuir-Blodgett-Kuhn (LBK) monolayers [49] present earlier attempts to construct supramolecular assemblies at the air-water interface. They embody critical handicaps compared to the natural membranes that inspired them, however, being rigid and inflexible, and suffering from stability issues that have limited the possibilities for scalability [50]. This work is suggestive of the use of soap films as viable alternatives, which can potentially overcome the bottlenecks encountered in LBK monolayers that precluded their widespread application. Soap films offer a unique range of compositional tunability, self-assembly, transport and interfacial properties, *and* scalability in the form of 3D soap foams or bubble-pair interfaces. They are fluid, dynamical mesoscopic structures capable of accommodating flexible supramolecular arrangements, making them more faithful representatives of their natural counterparts. Therefore, the fundamental finding of generating a symmetry-breaking arrangement in soap films can present a first step towards potential future applications, e.g., molecular sensors, chemically or optically triggered switches, opto-electronic devices, or asymmetrically arranged catalysts for solar energy conversion. It also suggests the possibility of using soap films as platforms for better understanding the structure and function of natural membranes.

All data are available in the main text or the Supplemental Material [23].

The authors would like to thank members of the SoFiA consortium for fruitful discussions. This project has received funding from the European Union's Horizon 2020 research and innovation program FETOPEN 2018-2020 under Grant Agreement No. 828838—SoFiA.

H. S. and N. K. carried out spectroscopic measurements and data analysis. N. K. performed surface tension measurements, and data visualization. L. H. conceptualized and guided the experiments. A. A. performed the synthesis and its validation. T. V. performed, validated, and visualized the coalescence measurements with the high-speed camera. E. C. conceptualized the modeling activities, L. B. and G. F. executed all modeling and computational work, validation, and data visualization. I. S. and E. C. conceived the doping methodology. C. R. provided the spray nozzle, high-speed camera, and their characterization. S. B. and A. A. contributed to the methodology. I. S. conceived the idea and found financial support. L. H., E. C., and S. B. supervised all research activities and found financial support.

All authors contributed to data interpretation and result presentation. N. K. wrote the manuscript with critical contribution from all co-authors.

Wasabi Innovations is a micro-industry partner in the SoFiA consortium and its associated commercial interests are protected by the published Bulgarian Patent No. BG67444B dated 15/06/2022. There are no related ethics issues. The authors declare no other competing financial interests.

*Corresponding author: eliodoro.chiavazzo@polito.it

†Corresponding author: indraneel.sen@wasabi-innovations.eu

‡Corresponding author: bonnet@chem.leidenuniv.nl

§Corresponding author: leif.hammarstrom@kemi.uu.se

||These authors contributed equally to this work.

- [1] H. Weyl, *Symmetry* (Princeton University Press, Princeton, NJ, 1952).
- [2] Y. Nambu and G. Jona-Lasinio, Dynamical model of elementary particles based on an analogy with superconductivity. I*, *Phys. Rev. B* **122**, 345 (1961).
- [3] E. Noether, Invariant variation problems, *Transp. Theory Stat. Phys.* **1**, 186 (1971).
- [4] E. Noether, Invariante Variationsprobleme, *Nachr. Ges. Wiss. Gött. Math.-Phys. Klasse* **1918**, 235 (1918), <https://eudml.org/doc/59024>.
- [5] G. van Meer, B. de Kruijff, J. A. F. Op den Kamp, and L. L. M. van Deenen, Preservation of bilayer structure in human erythrocytes and erythrocyte ghosts after phospholipase treatment. A 31P-NMR Study, *Biochim. Biophys. Acta (BBA)—Biomembr.* **596**, 1 (1980).
- [6] S. G. Sprague, Structural and functional consequences of galactolipids on thylakoid membrane organization, *J. Bioenerg. Biomembr.* **19**, 691 (1987).
- [7] C. A. Curcio, K. R. Sloan, P. Orin, A. E. Hendrickson, and R. E. Kalina, Distribution of cones in human and monkey retina: Individual variability and radial asymmetry, *Science* **236**, 579 (1987).
- [8] E. R. Kupers, N. C. Benson, M. Carrasco, and J. Winawer, Asymmetries around the visual field: From retina to cortex to behavior, *PLoS Comput. Biol.* **18**, e1009771 (2022).
- [9] Leonardo da Vinci, *Codex Leicester: A New Edition*, edited by Domenico Laurenza and Martin Kemp (Oxford University Press, Oxford, 2019), Vol. 3.
- [10] J. A. F. Plateau, *Statique Experimentale et Theorique Des Liquids Soumis Aux Seules Forces Moleculaires* (Gauthier-Villars, Paris, 1873), Vol. 2.
- [11] *Isaac Newton's Papers & Letters on Natural Philosophy and Related Documents*, edited by I. B. Cohen (Harvard University Press, Cambridge, 1958).
- [12] S. Mariot, M. Pasquet, V. Klein, F. Restagno, and E. Rio, A new setup for giant soap films characterization, *Eur. Phys. J. E* **44**, 52 (2021).
- [13] A. V. Grosse, Soap bubbles: Two years old and sixty centimeters in diameter, *Science* **164**, 291 (1969).
- [14] L. Shen, F. Denner, N. Morgan, B. van Wachem, and D. Dini, Transient structures in rupturing thin films: Marangoni-induced symmetry-breaking pattern formation in viscous fluids, *Sci. Adv.* **6**, eabb0597 (2020).

- [15] Soap bubbles and thin films, in *Bubble and Foam Chemistry*, edited by R. J. Pugh (Cambridge University Press, Cambridge, England, 2016), pp. 84–111.
- [16] R. Gera *et al.*, Emergence of electric fields at the water- $C_{12}E_6$ surfactant interface, *J. Am. Chem. Soc.* **143**, 15103 (2021).
- [17] R. Kusaka, S. Nihonyanagi, and T. Tahara, The photochemical reaction of phenol becomes ultrafast at the air-water interface, *Nat. Chem.* **13**, 306 (2021).
- [18] G. Falciani, R. Franklin, A. Cagna, I. Sen, A. Hassanali, and E. Chiavazzo, A multi-scale perspective of gas transport through soap-film membranes, *Mol. Syst. Des. Eng.* **5**, 911 (2020).
- [19] G. Falciani, L. Bergamasco, S. A. Bonke, I. Sen, and E. Chiavazzo, A novel concept of photosynthetic soft membranes: A numerical study, *Discover Nano* **18**, 9 (2023).
- [20] G. Duplâtre, M. F. Ferreira Marques, and M. da Graça Miguel, Size of sodium dodecyl sulfate micelles in aqueous solutions as studied by positron annihilation lifetime spectroscopy, *J. Phys. Chem.* **100**, 16608 (1996).
- [21] K. K. Pandey, H. C. Joshi, and T. C. Pant, Migration effects on excitation energy transfer by decay analysis using a nanosecond fluorimeter, *Chem. Phys. Lett.* **148**, 472 (1988).
- [22] L. Stryer and R. P. Haugland, Energy transfer: A spectroscopic ruler, *Proc. Natl. Acad. Sci. U.S.A.* **58**, 719 (1967).
- [23] See Supplemental Material at <http://link.aps.org/supplemental/10.1103/PhysRevLett.132.028201> for materials and methods, supplementary text, figures, equations, tables and videos, which includes Refs. [24–45].
- [24] E. C. Wijaya, F. Separovic, C. J. Drummond, and T. L. Greaves, Micelle formation of a non-ionic surfactant in non-aqueous molecular solvents and protic ionic liquids (PILs), *Phys. Chem. Chem. Phys.* **18**, 24377 (2016).
- [25] J.-L. Pierson, J. Magnaudet, E. J. Soares, and S. Popinet, Revisiting the Taylor-Culick approximation: Retraction of an axisymmetric filament, *Phys. Rev. Fluids* **5**, 073602 (2020).
- [26] J. Zou, W. Wang, C. Ji, and M. Pan, Droplets passing through a soap film, *Phys. Fluids* **29**, 062110 (2017).
- [27] D. D'Angelo, S. Kooij, F. Verhoeven, F. Sonvico, and C. van Rijn, Fluorescence-enabled evaluation of nasal tract deposition and coverage of pharmaceutical formulations in a silicone nasal cast using an innovative spray device, *J. Adv. Res.* **44**, 227 (2022).
- [28] H.-J. Butt, K. Graf, and M. Kappl, *Physics and Chemistry of Interfaces* (John Wiley & Sons, New York, 2013).
- [29] W. Brown, R. Johnsen, P. Stilbs, and B. Lindman, Size and shape of nonionic amphiphile ($C_{12}E_6$) micelles in dilute aqueous solutions as derived from quasielastic and intensity light scattering, sedimentation, and pulsed-field-gradient nuclear magnetic resonance self-diffusion data, *J. Phys. Chem.* **87**, 4548 (1983).
- [30] B. L. Bales, L. Messina, A. Vidal, M. Peric, and O. R. Nascimento, Precision relative aggregation number determinations of SDS micelles using a spin probe. A model of micelle surface hydration, *J. Phys. Chem. B* **102**, 10347 (1998).
- [31] E. Sutherland, S. M. Mercer, M. Everist, and D. G. Leaist, Diffusion in solutions of micelles. What does dynamic light scattering measure?, *J. Chem. Eng. Data* **54**, 272 (2009).
- [32] N. J. Chang and E. W. Kaler, The structure of sodium dodecyl sulfate micelles in solutions of water and deuterium oxide, *J. Phys. Chem.* **89**, 2996 (1985).
- [33] L. Xu, F. Mallamace, Z. Yan, F. W. Starr, S. V Buldyrev, and H. Eugene Stanley, Appearance of a fractional Stokes–Einstein relation in water and a structural interpretation of its onset, *Nat. Phys.* **5**, 565 (2009).
- [34] M. Molotskii, I. Torchinsky, and G. Rosenman, Hertz model for contact of water droplet with superhydrophobic surface, *Phys. Lett. A* **373**, 804 (2009).
- [35] J. N. Israelachvili, Strength of van Der Waals attraction between lipid bilayers, *Langmuir* **10**, 3369 (1994).
- [36] J. Pang and G. Xu, Comparison of the influence of fluorocarbon and hydrocarbon surfactants on the adsorptions of SDS, DTAB and C12E8 at the air/water interface by MD simulation, *Chem. Phys. Lett.* **537**, 118 (2012).
- [37] L. Martínez-Balbuena, A. Arteaga-Jiménez, E. Hernández-Zapata, and C. Márquez-Beltrán, Applicability of the Gibbs adsorption isotherm to the analysis of experimental surface-tension data for ionic and nonionic surfactants, *Adv. Colloid Interface Sci.* **247**, 178 (2017).
- [38] N. E. Barlow, H. Kusumaatmaja, A. Salehi-Reyhani, N. Brooks, L. M. C. Barter, A. J. Flemming, and O. Ces, Measuring bilayer surface energy and curvature in asymmetric droplet interface bilayers, *J. R. Soc. Interface* **15**, 20180610 (2018).
- [39] S. Narayan, I. Makhnenko, D. B. Moravec, B. G. Hauser, A. J. Dallas, and C. S. Dutcher, Microscale investigation of binary droplet coalescence using a microfluidic hydrodynamic trap, *Langmuir* **36**, 9827 (2020).
- [40] I. Kim and X. L. Wu, Tunneling of micron-sized droplets through soap films, *Phys. Rev. E* **82**, 026313 (2010).
- [41] G. A. Bach, D. L. Koch, and A. Gopinath, Coalescence and bouncing of small aerosol droplets, *J. Fluid Mech.* **518**, 157 (2004).
- [42] M. Motaghian, R. Shirsavar, M. Erfanifam, M. Sabouhi, E. Van Der Linden, H. A. Stone, D. Bonn, and M. Habibi, Rapid spreading of a droplet on a thin soap film, *Langmuir* **35**, 14855 (2019).
- [43] R. Macháň and M. Hof, Lipid diffusion in planar membranes investigated by fluorescence correlation spectroscopy, *Biochim. Biophys. Acta—Biomembr.* **1798**, 1377 (2010).
- [44] D. Marsh, *Handbook of Lipid Bilayers* (CRC Press, Boca Raton, 2013).
- [45] L. Picas, F. Rico, and S. Scheuring, Direct measurement of the mechanical properties of lipid phases in supported bilayers, *Biophys. J.* **102**, L01 (2012).
- [46] M. Fedoseeva, R. Letrun, and E. Vauthey, Excited-state dynamics of rhodamine 6G in aqueous solution and at the dodecane/water interface, *J. Phys. Chem. B* **118**, 5184 (2014).
- [47] N. Klonis and W. H. Sawyer, Spectral properties of the prototropic forms of fluorescein in aqueous solution, *J. Fluoresc.* **6**, 147 (1996).
- [48] E. A. Slyusareva, M. A. Gerasimov, A. G. Sizykh, and L. M. Gornostaevev, Spectral and fluorescent indication of the acidbase properties of biopolymer solutions, *Russ. Phys. J.* **54**, 485 (2011).
- [49] H. Kuhn, Present status and future prospects of Langmuir-Blodgett film research, *Thin Solid Films* **178**, 1 (1989).
- [50] O. N. Oliveira, L. Caseli, and K. Ariga, The past and the future of Langmuir and Langmuir-Blodgett films, *Chem. Rev.* **122**, 6459 (2022).